A "Biomechatronic EPP" Upper-Limb Prosthesis Control Configuration and its performance comparison to other control configurations

Spiros Kontogiannopoulos, Georgios A. Bertos*, *Member, IEEE*, and Evangelos Papadopoulos, *Fellow, IEEE*

***Abstract*— Upper-limb prosthetic technology has significantly changed in recent years. The devices available and those under development, have progressed the state of the art considerably. However, most are based on velocity control and fail to activate the proprioception of the amputee, as they do not provide their user with adequate feedback. A novel control configuration called "Biomechatronic EPP" has been developed to overcome these shortcomings, which is based on the concept of the Extended Physiological Proprioception (EPP), an upper-limb prosthesis proven to be functionally superior to velocity control configurations. The performance of the "Biomechatronic EPP" is compared to that of three other control toplogies including: a "Classic EPP" controller, an "Unconnected" controller and an "EMG" controller. Fourteen able-bodied subjects engaged in a 1-D Fitts' Law style task, designed with the Psychophysics Toolbox, a free set of MATLAB®. Performance was evaluated using several measures. Overall, the experimental results show that the performance of "Biomechatronic EPP" is comparable to "Classic EPP" and superior to "Unconnected" and "EMG". The proposed Biomechatronic EPP control configuration is an alternative to various invasive and non-invasive sensory feedback control integration methods for prosthesis control.**

***Index Terms*—Artificial limbs, Upper-Limb Prosthetics, Prosthesis, Control, Extended Physiological Proprioception.**

I. Introduction

THE replacement of the human hand by a prosthesis is a truly challenging task due to the significant mechanical demands and constraints [1]. To address a variety of user needs and lifestyles, current upper-limb prosthetics comprise a number of functional (eg control, grasp patterns) and cosmetic enhancements (e.g. appearance). However, the most critical factor for the proper function and use of an upper limb is its control.

Of all prostheses, myoelectric devices have been the most extensively studied. Their development has led to their acceptance as a routine and valid option for many arm amputees [2]. Today, there are myoelectric control systems which can be programmed in the fitting stage to suit the needs of each particular client [3]. However, such devices are subject to the stochastic nature of the myoelectric signals and to noisy control signals. Furthermore, myoelectric devices lack of adequate sensory feedback mechanisms [4] [5]. These are two of the major drawbacks limiting prosthesis' performance [6].

The classic Extended Physiological Proprioception (EPP) control configuration, first noted by D.C. Simpson in 1974 [7], as a control scheme for upper-limb prostheses is superior to myoelectric control due to the direct mapping of velocity and force between the residual limb and the prosthesis [8]. The EPP can be thought best of as the extension of the operator's proprioception into the prosthesis, that is, the prosthesis becomes an extension of the amputee's self. As shown in Fig. 1, Bowden cables are fitted to surgically modified exteriorized muscles/tendons sites of the residual arm (cineplasty) in order to mechanically interconnect the prosthetic hand to the rest of the amputee's body [9-12]. However, this control configuration has the disadvantage that it is not aesthetic for the human user, it is subject to control constraints related to the direction of the movement, and finally, a post-amputation plastic surgery is required. These drawbacks led to the gradual abandonment of EPP.

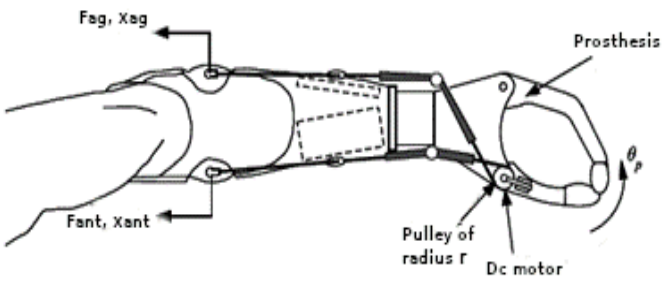

Fig. 1. "Classic EPP" control configuration (Adapted from [13])

*Corresponding author. Research supported in part by the EU Marie Sklodowska-Curie Career Integration Grant #334300.

Spiros Kontogianopoulos and Evangelos Papadopoulos are with the School of Mechanical Engineering, National Technical University of Athens (NTUA), Athens 15780, Greece (phone: +30-210-772-1440; fax: +30-210-772-1455; e-mail: spiroskont92@gmail.com, egpapado@central.ntua.gr). Georgios A. Bertos, was with the Biomedical Engineering Department, Northwestern University, Evanston, IL USA and the Rehabilitation Engineering Research Center, Northwestern University, 345 E. Superior, #1441, Chicago, IL 60611, USA. Now he is with the School of Mechanical Engineering, National Technical University of Athens, (email: gbertos@central.ntua.gr or george.bertos@gmail.com) and the Rehabilitation Engineering Research Center, Northwestern University, 680 N. Lake Shore Drive, Suite 1100, Chicago, IL, 60611-4496, USA.

Based on the master/slave architecture from the field of Telerobotics/Teleoperation [14], a new EPP-equivalent architecture was proposed in the Control Systems Laboratory of National Technical University of Athens (NTUA). This new control configuration, coined "Biomechatronic EPP", eliminates the drawbacks of the "Classic EPP" i.e. the needs for a cineplasty procedure and the use of Bowden cables [15]. The "Biomechatronic EPP" controller had been previously introduced as a microprocessor based "EPP" position controller; in a later study it was shown functionally equivalent to the "Classic EPP" [16]. In the same study [16], the real-time delay of the "Biomechatronic EPP Controller was approximately 78 ms, which corresponds to the delay between applying the force and the displacement of the slave motor. An initial thermal and power feasibility analysis of the "Biomechatronic EPP" control configuration was positive also [17].

According to the envisioned control configuration, low-power devices are to be implanted and connected to specific pair of agonist-antagonist muscles during or after the initial amputation surgery. Forces from the muscles of interest are exerted directly to the implants which play the role of the master robots of the teleoperation scheme. These forces are measured and used as input for the prosthesis, which is the slave robot of the system. The force measurements are wirelessly transmitted, while the controller of the control configuration achieves the dynamic coupling between the implanted motors and the prosthesis, providing this way the desired proprioceptive feedback to the amputee. The proposed control configuration is illustrated in Fig. 2. Before the miniaturized and biocompatible "Biomechatronic EPP" system shown in Fig. 2 is designed, verification and validation of the "Biomechatronic EPP" with appropriate target experiments is necessary in order to provide us with confidence of the quality of the proposed control configuration compared to traditional EPP and myoelectric control.

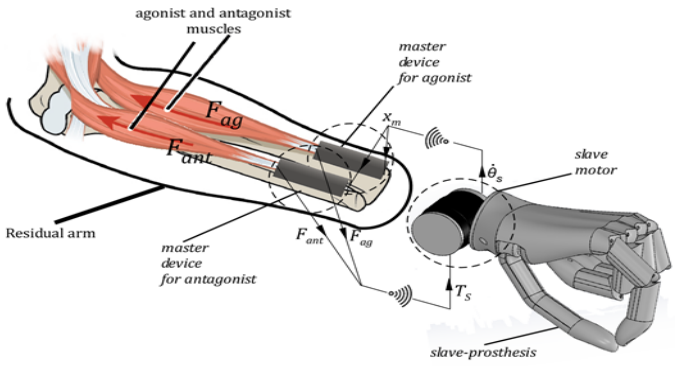

Fig. 2. Proposed control configuration of "Biomechatronic EPP".

In this paper, we present an experimental comparison amongst the proposed control configuration "Biomechatronic EPP", the "Classic EPP" control configuration, a torque controller without feedback, coined as "Unconnected" and the "EMG" control configuration.

The test used to experimentally compare the aforementioned control configurations was a target acquisition test, built accordingly to Fitts' Law, a physiological model of human movement which is employed extensively in the evaluation of Human Computer Interfaces (HCI). However, only recently biomedical applications have been shown to form a breeding ground for Fitts' Law testing [18].

It has been demonstated that the sense of touch and proprioception is of paramount importance for object manipulation in able-bodied subjects [19]. The restoration of the sensory feedback improves the motor control in terms of sensorimotor, coordination and dexterity performance [20-23] Different strategies have been presented to restore proprioceptive feedback in prosthetics: (a) the agonist-antagonist myoneural interface presented by Hugh Herr [24-26], where the natural agonist-antagonist pair is preserved during the amputation procedure, (b) the tendon vibration non-invasive technique used to elicit proprioceptive illusions [27, 28] which has been shown to restore proprioceptive information in amputees [29], (c) Electrical Nerve stimulation using implanted intraneural electrodes to provide one degree hand aperture feedback [30-32] or to provide sensory substitution as an alternative effective solution [33]. Additionally, researchers have demonstrated direct neural control of a multi-degree of freedom prosthesis using implanted peripheral electrodes [34, 35].

II. Methods

A. Experimental Setup

Fig. 3 shows the mechatronic setup used to prototype all four configurations. The dSpace DS1103 real-time controller, a legacy in rapid control prototyping, (A) in Fig. 3, was used for the implementation of the control configurations. The setup, see Fig. 3, also includes a slave (prosthesis) motor (D), corresponding to the slave motor in Fig. 3, a Bowden cable (C), corresponding to the cables in the "Classic EPP" cofiguration, and as an alternative to it, i.e. a set of two-master DC motors (B), connected to a set of screw-nut mechanisms and in-house fabricated housings equiped with force sensitive resistors (FSRs) and appropriate signal conditioning circuits (E), corresponding to the master devices in Fig. 3. A forearm cuff /pulley system, corresponding to the real muscles in Fig. 5 (discussed later), connects to the setup by pulling either the ends of the Bowden cable (C), or the FSR housings (E).

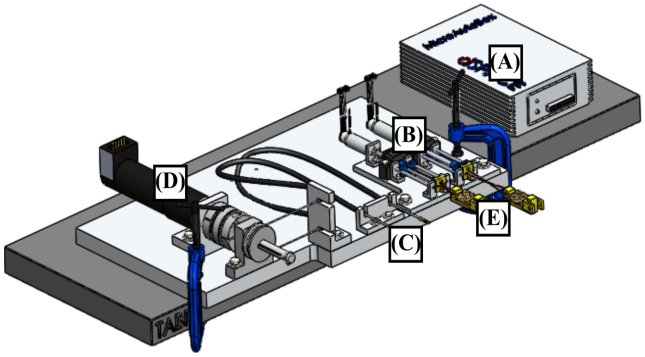

Fig. 3. The mechatronic prototype setup of all four configuration controllers. (A) dSPACE, (B) two master DC motors and screw-nut mechanisms, (C) Bowden cable, (D) slave (prosthesis) motor, and (E) housings with force sensitive resistors (FSRs).

Fig. 4 presents the "Biomechatronic EPP" control configuration in detail. The screw-nut mechanisms convert angular displacements to translations, and forces to torques. Their nuts are connected though inextensible strings to the FSR housings, which measure the forces applied to them. The user pulls the housings, through a forearm cuff/pulley system, the applied forces are measured by the FSR's, the slave motor rotates depending on the difference between the FSR applied forces, and the two master motors rotate so that the housings, through the screw-nut mechanisms yield to pulling. In other words, the command from the user to the prosthesis is a force command. The prosthesis transmits position feedback to the master motor's controller, which then affects the force feedback that the user feels via the leadscrews, providing this way the proprioceptive feedback, see Fig. 4 and Fig. 5. The master motors are commanded to follow the slave's angular motion via a low-power Bluetooth link.

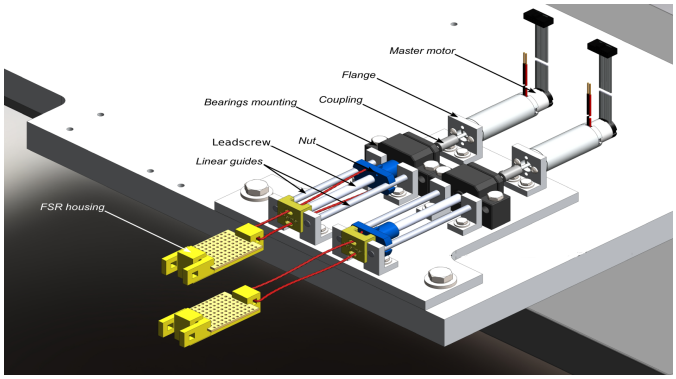

Fig. 4. "Biomechatronic EPP" setup showing the master motors, leadscrews and nuts, and FSR housings.

For the "Classic EPP", the master motors are not used. Instead, the connection between the user force input and the slave (prosthesis) motor is achieved mechanically via the Bowden cable and slave motor pulley, Fig. 3 (C), i.e. the user receives proprioceptive feedback through the Bowden Cable directly coupled to the prosthesis via the slave motor pulley.

In the "Unconnected" control configuration, the user force input drives the slave motor, but there is no direct connection between them; i.e. no feedback is provided to the user.

In the "EMG" control configuration, the reference input is provided by myoelectric signals, acquired from the muscles of interest via the Myo Armband, by Thalmic Labs. Again, in this case no feedback is provided to the user.

To map an isolated movement of the wrist-flexion extension of the physiological limb to the opening and closing of the prosthesis, a forearm cuff (orthosis) was used, which allowed only wrist flexion and extension. The forearm cuff was used in all four different experimental configurations in order to increase repeatability. For the "Classic EPP", the "Biomechatronic EPP" and the "Unconnected" control configurations, the forces excreted by the user during the flexion and the extension of its wrist were transmitted to the FSR sensors, (b) in Fig. 5, via inextensible miniropes and forearm cuff/pulley system (a) in Fig. 5. A control system that reads these forces commanded the prosthetic (slave) motor to move the prosthetic limb attached to it. For the "EMG" control configuration, the subject used both the cuff and Myo Armband (c) in Fig. 5.

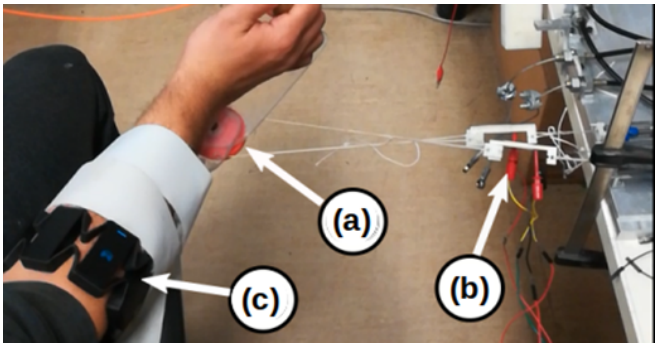

Fig. 5. A subject during the experiment. (a) system of miniropes connected to FSRs and forearm cuff (orthosis)/pulley system, (b) FSRs (c) Myo Armband.

B. Control configurations

The command input for the "Biomechatronic EPP", "Classic EPP" and "Unconnected" control configurations is the difference between the forces recorded by the FSR sensors. The control scheme for these control configurations is presented in Fig. 6. The blocks inside the red box are used as controller for the "Classic EPP" and "Unconnected" schemes. The signal provided by the FSR sensors ranges between 0V and +5V. The dead zone block models the threshold below which the measured force does not trigger motion to the corresponding limb, while the saturation block is used as a protection in case the input exceeded the predetermined levels. The absolute difference between the two antagonist forces is then normalized to represent the duty cycle of the PWM signal which is required as input for the slave motor driver, to control the velocity of the prosthesis. The prosthesis motion direction is determined by the sign of the force difference.

In "Biomechatronic EPP" control configuration, the angular position (θ) of the slave motor is translated to linear displacement (x) and serves as input to the PD controllers of the two master motors. To imitate the proprioception provided by the Bowden cables in the "Classic EPP" configuration, the power screws of the master motors move along their axes in opposite direction. Apart from the PD controllers, feedforward friction compensation is used so as to enhance the tracking performance of the master motors [36]. The design of the closed loop control scheme for the "Biomechatronic EPP" was part of a previous related study [37]. In the case of the "Classic EPP", the proprioception of the user is preserved via the Bowden cables, while in the case of the "Unconnected" method, no feedback is provided.

In the "EMG" control configuration, surface EMG signals are collected from Extensor Carpi Radialis (wrist extension) and Flexor Carpi Radialis (wrist flexion) using the Myo Armband. The range of potentials provided by the Myo armband is between -128 and 128 in units of activation [38]. The EMG data is streamed at 200Hz. Myo has also an in-built antialiasing filter and a Notch filter at 50Hz. The EMG signals were then passed into MATLAB® for further processing.

The controller employed is shown in Fig. 7. The collected signals are high-pass filtered, rectified, and low-pass filtered.

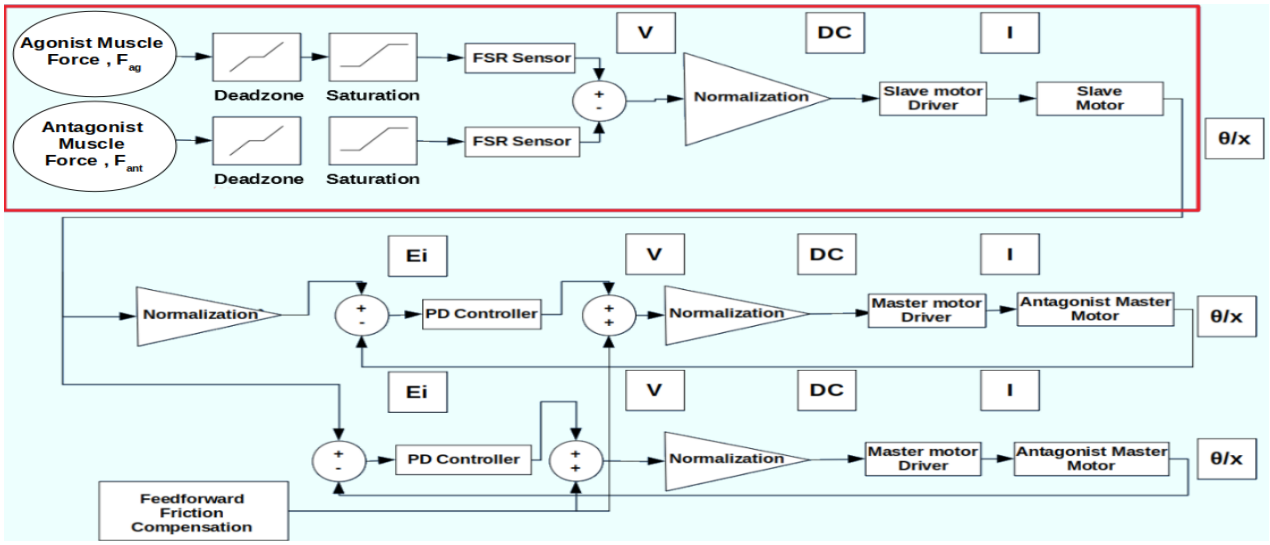

Fig. 6. Control scheme for "Biomechatronic EPP". The blocks inside the red box are used as controller for the "Classic EPP" and "Unconnected" schemes.

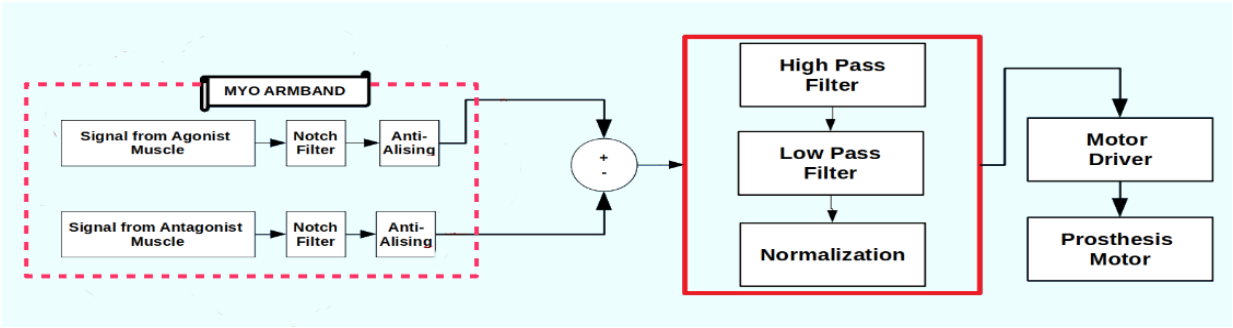

Fig. 7. "EMG" control scheme. EMG signals from a pair of antagonist muscles are recorded with Myo Armband and processed in Matlab Simulink® as shown. A signal proportional to the difference between them is provided to the motor driver.

Both the high pass and low pass filters used were fourth order Butterworth filters with cutoff frequencies at 30 Hz and 6 Hz respectively. The filters were designed according to [39]. The mean absolute values (MAVs) of the EMG signals were calculated from 100 ms sliding windows, with a frame increment of 50 ms. The MAVs of the antagonistic pair were normalized using the method of Maximum Voluntary Isometric Contraction (MVIC), and thresholds were applied [40]. The difference in signal amplitude was then determined and used to set the duty cycle of the motor driver. More explicitly, this difference is given by:

$$\%DC = \left| \left[M_1 / G_1 - T_1\right] - \left[M_2 / G_2 - T_2\right] \right| \times 100\% \quad (1)$$

where M_1 is the MAV of the first muscle in the antagonistic pair, G_1 is the respective value obtained during MVIC, and T_1 is the threshold applied. Similarly, M_2, G_2, and T_2 represent the second muscle MAV, MVIC value, and threshold. Thresholds are set manually to minimize unintended activity.

C. *Fitts' Law*

Fitts' law is a model of human psychomotor behavior based on Shannon's Theorem, a fundamental theorem of communication systems [41]. Fitts reasoned that a human operator that acquires targets over a certain amplitude (signal), and with variable success (noise), essentially is demonstrating a "rate of information transfer" [42]. Fitts' Law Test has become an international standard (ISO9241-9) for the validation of practically any type of human-computer interface (HCI) including mice, joysticks, touchpads, and even eye trackers [43].

Lately, several studies have extended the use of Fitts' Law as a performance model for different upper limb control configurations [44] [45] [46] [47] [48]. According to Fitts' Law, in target acquisition tasks there is a speed and accuracy trade-off which is defined by:

$$MT = a + b \times ID \quad (2)$$

where *MT* is the time (in seconds) required to reach a target, *a* and *b* are the regression coefficients, and *ID* is a target's index of difficulty (in bits).

The *ID*-term in (2) expands as follows:

$$ID_e = \log_2\left(D/W + 1\right) \quad (3)$$

where D and W are the target distance and width, respectively. Fitts proposed a metric initially called *index of performance* (*IP*), now *throughput* (*TP*), to quantify the human performance in the context of the task, device, and environmental conditions, when each experiment is performed [49]. The thoughput *TP* is calculated by:

$$TP = ID / MT \quad (4)$$

In this stydy, an alternative method, called *adjustment for accuracy* was implemented to calculate *TP*. This method was

initially proposed by Crossman as a means to account for a subject's accuracy [50, 51]. As described by Soukoreff & Mckenzie, this technique proposes the use of the effective width (W_e) and distance (D_e) instead of the target's actual width and distance [52], in order to include spatial variability or accuracy in the calculation. The W_e is computed as 4.133×SD, where SD is the selected coordinates standard deviation, and D_e is the mean of the actual movement amplitudes in the sequence of trials.

Using the effective values, a task's effective index of difficulty can then be defined as:

$$ID_e = \log_2\left(D_e / W_e + 1\right) \quad (5)$$

Subsequently, the TP is calculated as:

$$TP = ID_e / MT \quad (6)$$

where MT is now the mean movement time (in seconds), recorded over a sequence of trials. Testing over two or three separate test conditions, the differences in TP can be used to assess performance differences between the conditions. This is also in agreement with [8].

D. Target Experiments

To imitate the movement a hand makes during flexion and extension, a 3D-printed rectangular link (shaft) was added to the gearhead of the slave (prosthesis) motor (see Fig. 8). The bounds of the wrist movement were modeled by adding two mechanical stops restraining the link motion, the first at 90 degrees in the clockwise direction and the second at 75 degrees in the counterclockwise direction. Thus, the 3D-printed link emulates the role of the prosthetic limb, and the slave (prosthesis) motor of the prosthetic limb actuator.

The goal of the experiment was to determine the ability of the subjects to manipulate the displacement of the slave motor and link using the four aforementioned control configurations.

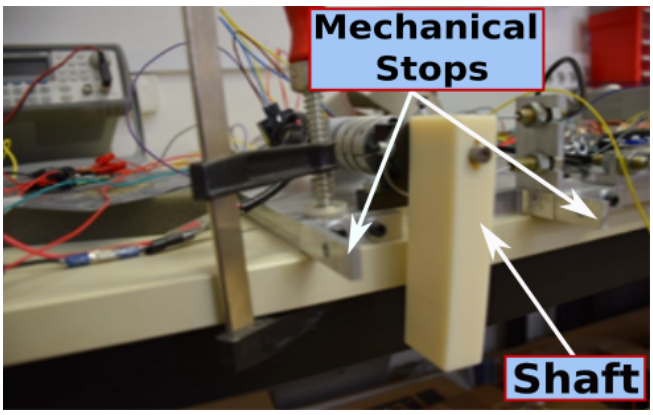

Fig. 8. Shaft (here in vertical position) added to imitate wrist movement and the mechanical stops of the setup.

1) Subjects

Fourteen able-bodied subjects participated in this study. Of them 12 were male and 2 female, and ranged in age between 20 and 33. The subjects signed an IRB form which contained the description of the experiment and all the risks involved.

2) Procedure

The task was designed to be similar to Fitts' original serial task [42]. A monitor was used to display the current position of the prosthesis link by means of the position of a cross cursor, see Fig. 9. The subjects performed reciprocal pointing on the pair of targets provided. The targets were limited to one DoF and appeared on the periphery of a green semicircle, which corresponded to the link endpoint orbit. Their position was described by their central angle with respect to the semicircle. The grey circular target corresponds to the starting point and the red to the target point (see Fig. 9).

Subjects were asked to move the cursor (black cross) to the location of the target circle and remain within the width of the target for the predetermined dwell time (1 s). The subject was guided through the block of trials by intechanging the colors of the targets. Participants were instructed to acquire the targets as quickly and accurately as possible. If too many errors were made, they were instructed to move slower, while if they never (or rarely) made an error, they were instructed to move faster. Each subject was given one warm-up block of trials prior to data collection, for each unique control configuration.

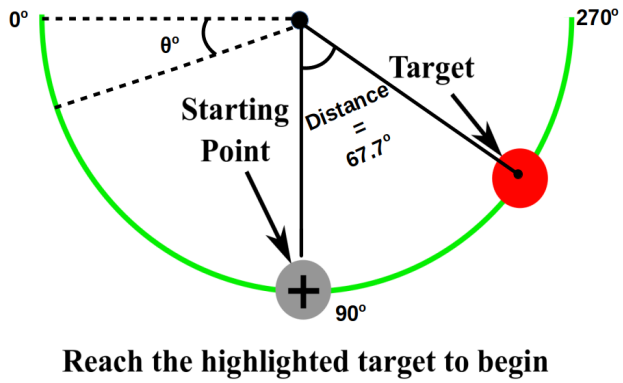

Fig. 9. Monitor display during the experiment. The grey circle is the starting point, and the red the target point. The cross is at the starting point.

3) Design

A within-subjects design was used. Independent variables were the control configuration (four levels), the task (one level), the target distance (five levels), and the target width (five levels). TABLE I details the combinations of the target widths (W) and distances (D) and the resulting indices of difficulty (ID) used in the experiment.

The experiment was structured by trials, blocks and sessions. Trial was a single target-select task, block was a group of 15 trials for the same target-select task, and session was a group of 25 random blocks (each block represented one different combination of distance and target width) in descending order of target widths.

Different control configuration sessions were conducted on four separate days for each subject, since only one was done in one day. The order was randomized. After the completion of the required experiments for all control configurations, one subject had completed 1500 trials (15 × 5 × 5 × 4).

TABLE I
Combinations of widths (W) and distances (D) and resulting Indices of Difficulty (ID)

W (°)	D (°)				
	27.5	**67.7**	**80**	**90**	**135**
2	3.88	5.12	5.36	5.60	6.10
3	3.34	4.56	4.80	5.03	5.52
5	2.70	3.86	4.09	4.32	4.81
10	1.91	2.95	3.17	3.39	3.86
15	1.50	2.46	2.67	2.87	3.32

E. Performance Metrics

Although *TP* provides a useful over-all measure of performance, metrics of *movement time* (*MT*) and *error rate* (*ER*) (calculated from the reaching central angle) were also calculated to complete the picture [53]. The movement time was measured from the beginning of a move to the reaching of a target (dwell time and reaction time excluded from the measurement of movement time). The beginning of a new movement occurred with the first cursor position change following the end of the previous one. The error rate was computed using the following formula:

$$\%ER = \frac{\#Trials - \#Hits}{\#Trials} \times 100\% \quad (7)$$

A trial was claimed as a "Hit" only if the subject managed reaching the target and remaining inside it for 1s (dwell time), as it has been previously mentioned. An error was defined as overshooting the target, when the subject had managed reaching the target but not remain inside it long enough. No corrective movement was allowed. The next movement was initiated from the point at which the last one had terminated.

F. Statistical Analysis

Analysis of all collected data was conducted using MATLAB®. Tests for main effects of the control configuration on three dependent variables; *MT*, *ER* and *TP* were conducted using *one-way analysis of variance* (one-way ANOVA) to determine whether there were any statistical significant differences between the means of the four independent control configurations. Significance was assessed at a = 0.05 and a = 0.01, and Bonferroni corrections were applied to post-hoc comparisons. The overall significance of linear regression models was determined using an F-test.

Prior to using ANOVA for the statistical analysis of the acquired data, a Kolmogorov-Smirnov test was employed to evaluate the normality for all data sets. All data sets proved to be no signifficantly different from being normally distributed.

No significant outliers were observed amongst the subjects. It is important to note that in our previous statistical analysis, we performed a data analysis in order to remove possibly misfired individual trials. We considered as outliers the trials in which a subject either was hurried and started the next movement before dwell time was completed - even if he or she had reached the previous target successfully - (spatial outliers) or paused mid-trial violating the rules that the movements had to be rapid (timing outliers).

III. Results

Fig. 10 displays the relationship between movement time (*MT*) and effective index of difficulty (ID_e). Data was averaged across all subjects for all twenty-five experimental blocks. The R^2 values (coefficient of determination) for the linear regression models, ranged between 0.902 and 0.969, indicate strong linear relationship supporting the validity of applying Fitts' Law model [54]. More precisely, *MT* and ID_e were found to be strongly correlated for all control configurations, "Biomechatronic EPP" - r(22) = 0.969, p<0.01, "Classic EPP" - r(22) = 0.984, p<0.01, "Unconnected" - r(22) = 0.982, p<0.01, "EMG" - r(22) = 0.950, p<0.01.

Fig. 11 and TABLE II summarize the performance (mean ± standard deviation) of each control configuration across the various performance metrics. The grand mean for movement time was 1.73 s. Across the control configuration factor, the means for "Biomechatronic EPP", "Classic EPP", "Unconnected" and "EMG" were 1.63 ± 0.3, 1.72 ± 0.4, 1.68 ± 0.3 and 1.89 ± 0.4 s. The p-value corresponding to the F-statistic of one-way ANOVA was higher than 0.05 ($F_{3,52}=1.399$, $p>0.05$) suggesting that there was not significant effect of the control configuration on movement time.

TABLE II
Summary of the performance metrics

	MT (s)	**Error (%)**	**TP (bits/s)**
"Biomechatronic EPP"	1.63 ± 0.3	13.2 ± 7.8	2.461 ± 0.398
"Classic EPP"	1.72 ± 0.4	19.3 ± 11.2	2.402 ± 0.547
"Unconnected"	1.68 ± 0.3	44.3 ± 13.9	2.000 ± 0.388
"EMG"	1.89 ± 0.4	56.0 ± 9.3	1.589 ± 0.419

An error was defined as overshooting the target. The grand mean of error rate was 33.2%. The error rates were $13.2 \pm 7.8\%$, $19.3 \pm 11.2\%$, $44.3 \pm 13.9\%$, and $56.0 \pm 9.3\%$, for "Biomechatronic EPP", "Classic EPP", "Unconnected" and "EMG", respectively. There was no significant difference on error rate between "Biomechatronic EPP" and "Classic EPP" ($p>0.05$). Subjects made more overshoots using the "Unconnected" control configuration compared to "Biomechatronic EPP" ($p<0.01$) and "Classic EPP" ($p<0.01$). The error rate was also greater for "EMG" compared to "Unconnected" ($p<0.05$).

The "Biomechatronic EPP" *TP* (2.461 ± 0.398bits/s) was significantly greater than both "Unconnected" ($p<0.01$) and "EMG" ($p<0.01$). However, there was no statistical difference between "Biomechatronic EPP" and "Classic EPP" ($p>0.05$). Subjects presented better performance using "Classic EPP" than "EMG" ($p<0.01$), while the Throughput (*TP*) was statistically the same for the pairs of "Classic EPP"-"Unconnected" ($p>0.05$) and "Unconnected"-"EMG" ($p>0.05$).

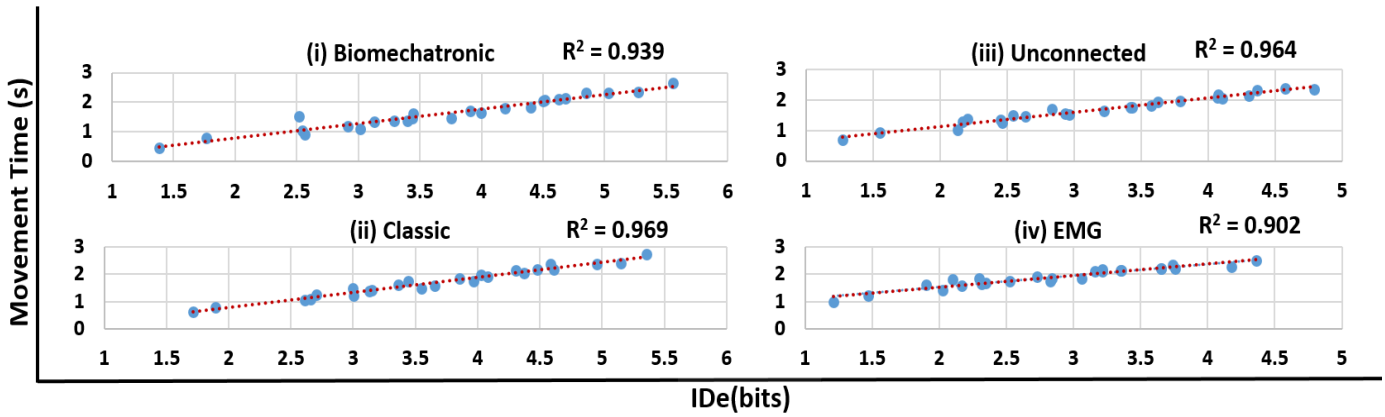

Fig. 10. Relationship between movement time (MT) and effective index of difficulty (IDe) for "Biomechatronic EPP", "Classic EPP", "Unconnected" and "EMG".

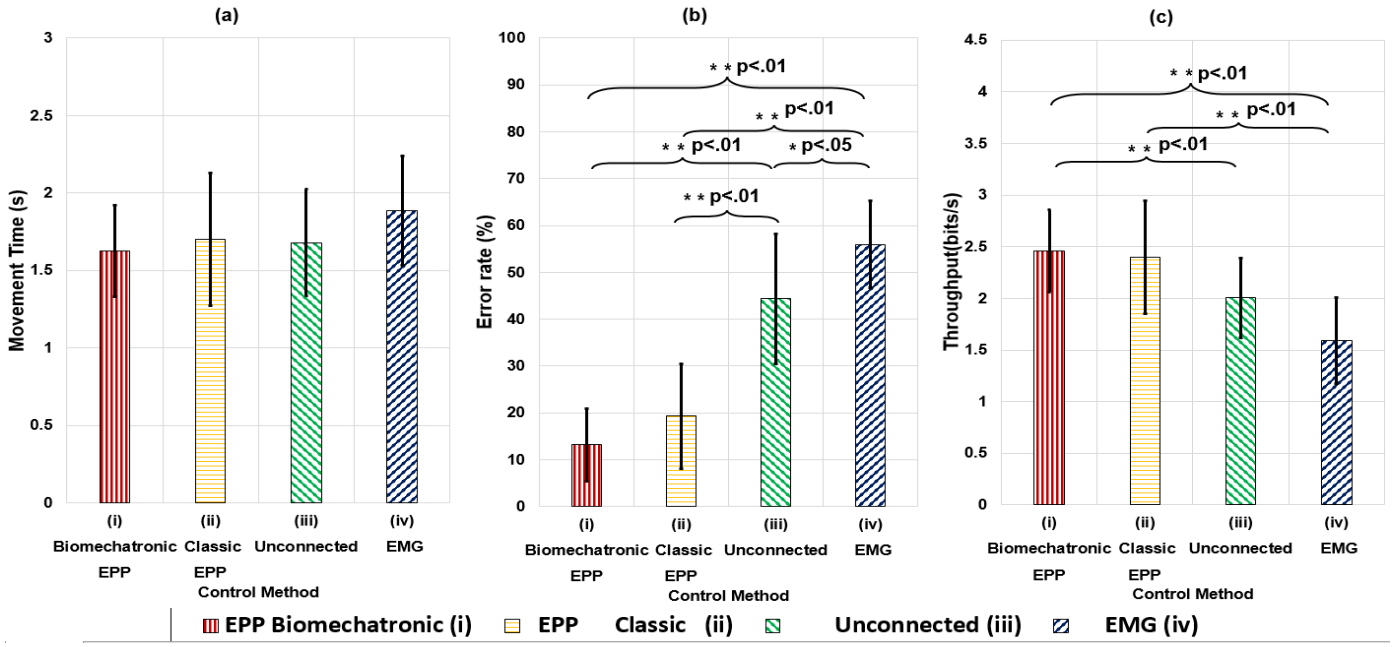

Fig. 11. Performance of control configurations across the various performance metrics (a) Movement time (b) Error rate (c) Throughput. Pairwise comparisons are noted with brackets. Errorbars indicate standard deviations. Symbols * and ** denote a significant difference at .05 and .01 significance level, respectively.

IV. Discussion

The use of EPP as a control scheme for upper-limb prostheses has declined over the last decades; surface EMG has been the standard for clinically available prosthetic devices due to its non-invasiveness and easiness to apply.

In this study a comparative assessment was made of "Biomechatronic EPP", a novel upper-limp control configuration, "Classic EPP", "Unconnected" and "EMG" control configurations. This investigation was made in the context of a real time, computer based, target acquisition test using a Fitts' law approach. High R^2 values obtained from regression plots (Fig. 10) support the notion that Fitts' law framework is a viable testing tool for these upper-limb prostheses evaluation. More specifically, these results confirm the suitability of Fitts' law for the assessment of myoelectric control schemes, previously reported in related studies [18, 48, 55], while they set also the basis for its use with EPP based control configurations.

As its calculation includes both speed (*MT*) and accuracy (*ER*), *TP* is indicative of the overall performance. Based on the results exported from a one-way ANOVA parallel with the applied Bonferroni corrections for this metric, the superiority of "Biomechatronic EPP" over the "Unconnected" control configuration and the "EMG" based control was revealed. On the other hand, no significant difference was observed in the performance of the subjects during the "Biomechatronic EPP" and "Classic EPP" sessions of the experiment. This indicates the statistical equivalence of these control techniques and supports the results derived from our previous study [16].

When looking at the performance metric of movement time, no statistically significant difference is revealed across all control configurations. However, the duration of the movement, by its own, is not wholly indicative of the usability of a control configuration. Lower movement time, for example, corresponds to higher speed which may cause the prosthesis to move further in the wrong direction. The picture becomes clearer, if we take into account the second descriptive metric used, the Error Rate. Here, the analysis gave us unambiguous results. In terms of the

Error Rate, the "Biomechatronic EPP" significantly outperforms the "Unconnected" and "EMG" control configurations while has statistically equal performance ($p>0.05$) to "Classic EPP" configuration. This is illustrative of the subjects' ability to acquire the target effectively.

Given the statistically same results in movement time, the differences mentioned in Error Rate among the control configurations contributed the most to the results in Throughput, and subsequently in the overall performance.

Concluding, the absence of proprioceptive feedback during the sessions of "Unconnected" and "EMG" control configurations seems to be the main reason for their poor performance. Especially for the "EMG" based scheme, the majority of the subjects reported frustration, describing loss of control, especially when they were close to the target and more precise movements required. This may have been caused by the lack of the subjects' prior experience with "EMG" based experiments, which require high concentration. Another reason might be the limitations of the Myo Armband. It has been observed that we were only receiving EMG measurements with a somewhat irregular sample-rate over the BLE interface. The actual rate was found to vary between 175 Hz and 185 Hz, and not reaching the 200 Hz specified in the data sheet. However, unintended or unstable muscle activation are generally justified by the stochastic nature of the EMG signals. On the other hand, the "Biomechatronic EPP" configuration managed to provide the users with the adequate sensory feedback of the "Classic EPP" scheme, leading to more precise and smoother control of the prosthesis.

It has to be noted that while this study has shown encouraging results, it is only the second step in our analysis. The first step was the development of the equivalent to Classic EPP [13] proposed "Biomechatronic EPP" architecture [15], along with some preliminary feasibility analysis [56]. The second step is the work presented in this study, which is the verification and validation with experiments that the proposed architecture is equivalent to the traditional EPP and is superior to myoelectric control. Our third step is a combination of advanced feasibility and miniaturization design in order for the slave robots to be implanted in vivo in patients and overcome problems such as reliability, biocompatibility, size of sufficient battery and motor. We cannot spend a lot of effort on the third step without having a positive outcome of the first and second steps. As a first step, we applied the Biomechatronic EPP concept for one degree of freedom (flexion / extension of the wrist) at the transradial level. We envision that this work is the building block, which if scaled up could be applied appropriately for transhumeral amputations or of various degrees of freedom of the arm.

Lately, there have been a lot of methods proposed for controlling multi-degree of freedom prostheses. There is the idea to control via the brain interface [57] using Brain Machine Interface via a chip implant, which is not the right methodology for amputees, but for tetraplegic patients.

Implantable Myoelectric Sensors (IMES), is a technique that uses miniature BIONs to be implanted in the musculature of the amputee in order to acquire myoelectric signals of both efferent and afferent intent to improve the control scheme by adding feedback [58, 59]. A variation of this technique is using TIME electrodes [60]. Similarly to TMR, a multi-dimensional machine learning block with pattern recognition techniques are needed in order to control a multi-degree of freedom prosthesis.

Osseointegration, similarly to EPP, takes advantage of a natural and existing proprioceptive channel to augment the control quality of upper and lower limb amputees by enhancing the proprioceptive feedback transmitted via the implant which is rigidly integrated with the amputee's bone [61].

Targeted Muscle Reinnervation (TMR) is a surgical technique [62], that is useful for cases where there are not enough control sites for prosthesis control, which might be the case during short amputations (eg short transhumeral amputation) and/or multi-degree of freedom prosthesis control. It is found that during the sensory reinnervation, the sensory information and feedback of the nerve is preserved in the new hosted muscular site [62]. Nevertheless, a multi-dimensional controller using novel artificial intelligence techniques is needed for deciphering the intent of movement and provide appropriate feedback to the amputee.

Regenerative Peripheral Nerve Interfaces (RPNI) are surgical procedures which are useful to innervate denervated muscles that can then control a prosthesis [63], with advantages and disadvantages similar to TMR.

The Implanted Magnets solution [64], proposes the use of miniature magnets which are implanted in the muscles and their relative position is acquired via an external tracking system. This method is fairly new, with no proven quality comparison to other control configurations and confidence for a good quality for multi-degree of freedom prosthesis control. This solution requires extra steps to go from magnet position to length change of muscle and transformation of that intent of movement even for a one degree of freedom solution. For multi-degree of freedom solution,

Similar to the Implanted Magnets solution, there is the genetic marking and use of visual read to decipher the activation of a particular muscle or group of muscle fibers in order to command a prosthesis [65]. This is a fairly new technology, with advantages and disadvantages similar to the Implanted Magnets solution.

The "Biomechatronic EPP" takes advantage of the fact that the "amplifier" of the neuromuscular system - the muscle and tendon - is intact for many muscles of the amputated patients. By integrating the slave robots to these "amplifiers," we omit the issues of low signal to noise ratio that IMES, or the Myokinetic Control Interface might have. The proprioceptive feedback is inherent in EPP and to Biomechatronic EPP, therefore we do not have to solve the problem of modeling of the afferent and efferent signals from neurons like other methods, like IMES might have. These other alternatives have to synthetically integrate to the human proprioceptive feedback system. On contrary, integration to the EPP control configurations is intuitive and part of the command channel which also serves as the proprioceptive. Of course, we have other challenges with the Biomechatronic EPP, such as implant

size, power and biocompatibility; for which we hope to solve creatively in the near future.

V. Conclusion

The study presented here, reveals the supriority of "Biommenchatronic EPP" over the "Unconnected" and EMG control configurations in both terms of Error Rate ($p<0.01$) and Throughput ($p<0.01$), while its performance proved to be equivalent to that of "Classic EPP". The results are encouraging and lead us to invest more in this control configuration, which in the future can become the core of many DOFs prosthetic systems. The proposed EPP control configuration restores the idea of user proprioception in upper-limb prosthetics. We truly believe that this is a promising novelty and has the potential to ameliorate the life of perspective amputees. A physically implemented miniaturized biocompatible "Biomechatronic EPP" prototype is our next goal.

Acknowledgment

The authors would like to thank John W. Michael, MEd, CPO of Northwestern University Prosthetics Orthotics Center, for designing and fabricating the forearm cuff mechanism used during the experiments. Additionally, they thank Nicholas Hatsopoulos of University of Chicago for an insightful discussion on target experiments.

References

[1] G. A. Bertos and E. G. Papadopoulos, "Chapter Six - Upper-Limb Prosthetic Devices," in *Handbook of Biomechatronics*, J. Segil, Ed.: Academic Press, 2019, pp. 177-240.

[2] L. McLean and R. N. Scott, "The Early History of Myoelectric Control of Prosthetic Limbs (1945–1970)," in *Powered Upper Limb Prostheses: Control, Implementation and Clinical Application*, A. Muzumdar, Ed. Berlin, Heidelberg: Springer Berlin Heidelberg, 2004, pp. 1-15.

[3] D. F. Lovely, "Signals and Signal Processing for Myoelectric Control," in *Powered Upper Limb Prostheses: Control, Implementation and Clinical Application*, A. Muzumdar, Ed. Berlin, Heidelberg: Springer Berlin Heidelberg, 2004, pp. 35-54.

[4] B. Peerdeman *et al.*, "Myoelectric forearm prostheses: state of the art from a user-centered perspective," *J Rehabil Res Dev,* vol. 48, no. 6, pp. 719-37, 2011.

[5] C. Antfolk, M. D'Alonzo, B. Rosen, G. Lundborg, F. Sebelius, and C. Cipriani, "Sensory feedback in upper limb prosthetics," *Expert Rev Med Devices,* vol. 10, no. 1, pp. 45-54, Jan 2013.

[6] E. A. Biddiss and T. T. Chau, "Upper limb prosthesis use and abandonment: a survey of the last 25 years," *Prosthet Orthot Int,* vol. 31, no. 3, pp. 236-57, Sep 2007.

[7] D. C. Simpson, "The choice of control system for the multimovement prosthesis: extended physiological proprioception (EPP)," in *The Control of Upper-Extremity Prostheses and Orthoses*, e. a. Herberts, Ed.: Springfield, IL: Thomas, 1974, pp. 146-150.

[8] J. A. Doubler and D. S. Childress, "Design and evaluation of a prosthesis control system based on the concept of extended physiological proprioception," *J Rehabil Res Dev,* vol. 21, no. 1, pp. 19-31, May 1984.

[9] P. E. Klopsteg and P. D. Wilson, *Human Limbs and their substitutes*, 2nd Edition ed. New York: McGraw-Hill, 1954.

[10] R. F. Weir, C. W. Heckathorne, and D. S. Childress, "Cineplasty as a control input for externally powered prosthetic components," *Journal of Rehabilitation Research and Development,* Article vol. 38, no. 4, pp. 357-363, Jul-Aug 2001.

[11] M. Tavakoli, J. Lourenço, and A. T. d. Almeida, "3D printed endoskeleton with a soft skin for upper-limb body actuated prosthesis," in *2017 IEEE 5th Portuguese Meeting on Bioengineering (ENBENG)*, 2017, pp. 1-5.

[12] P. Tropea, A. Mazzoni, S. Micera, and M. Corbo, "Giuliano Vanghetti and the innovation of "cineplastic operations"," *Neurology,* vol. 89, no. 15, pp. 1627-1632, Oct 10 2017.

[13] Y. A. Bertos, C. W. Heckathorne, R. F. Weir, D. S. Childress, and I. Ieee, "Microprocessor based e.p.p. position controller for electric-powered upper-limb prostheses," in *Proceedings of the 19th Annual International Conference of the Ieee Engineering in Medicine and Biology Society, Vol 19, Pts 1-6 - Magnificent Milestones and Emerging Opportunities in Medical Engineering*, vol. 19(Proceedings of Annual International Conference of the Ieee Engineering in Medicine and Biology Society, New York: Ieee, 1997, pp. 2311-2314.

[14] Y. Yokokohji and T. Yoshikawa, "Bilateral control of master-slave manipulators for ideal kinesthetic coupling-formulation and experiment," *IEEE Transactions on Robotics and Automation,* vol. 10, no. 5, pp. 605-620, 1994.

[15] A. Mablekos-Alexiou, G. A. Bertos, and E. Papadopoulos, "A Biomechatronic Extended Physiological Proprioception (EPP) Controller for Upper-Limb Prostheses," in *2015 IEEE/RSJ International Conference on Intelligent Robots and Systems (Iros),* pp. 6173-6178, 2015.

[16] S. Kontogiannopoulos, Z. Vangelatos, A. G. Bertos, and E. Papadopoulos, "A Biomechatronic EPP upper-limb prosthesis controller and its performance comparison to other topologies," in *40th International IEEE Engineering in Medicine and Biology Conference*, Honolulu, Hawaii, USA, July 17-21, 2018, 2018.

[17] E. Moutopoulou, G. A. Bertos, A. Mablekos-Alexiou, and E. G. Papadopoulos, "Feasibility of a biomechatronic EPP Upper Limb Prosthesis Controller," in *2015 37th Annual International Conference of the IEEE Engineering in Medicine and Biology Society (EMBC)*, 2015, pp. 2454-2457.

[18] J. Gusman, E. Mastinu, and M. Ortiz-Catalan, "Evaluation of Computer-Based Target Achievement Tests for Myoelectric Control," *IEEE J Transl Eng Health Med,* vol. 5, p. 2100310, 2017.

[19] R. S. Johansson and J. R. Flanagan, "Coding and use of tactile signals from the fingertips in object manipulation tasks," *Nature Reviews Neuroscience,* vol. 10, no. 5, pp. 345-359, May 2009.

[20] D. W. Tan, M. A. Schiefer, M. W. Keith, J. R. Anderson, J. Tyler, and D. J. Tyler, "A neural interface provides long-term stable natural touch perception," *Sci Transl Med,* vol. 6, no. 257, p. 257ra138, October 8, 2014.

[21] G. Valle *et al.*, "Biomimetic Intraneural Sensory Feedback Enhances Sensation Naturalness, Tactile Sensitivity, and Manual Dexterity in a Bidirectional Prosthesis," *Neuron,* vol. 100, no. 1, pp. 37-45 e7, Oct 10 2018.

[22] F. Clemente *et al.*, "Intraneural sensory feedback restores grip force control and motor coordination while using a prosthetic hand," *Journal of Neural Engineering,* vol. 16, no. 2, Apr 2019.

[23] F. M. Petrini *et al.*, "Six-Month Assessment of a Hand Prosthesis with Intraneural Tactile Feedback," *Ann Neurol,* vol. 85, no. 1, pp. 137-154, Jan 2019.

[24] T. R. Clites, M. J. Carty, S. Srinivasan, A. N. Zorzos, and H. M. Herr, "A murine model of a novel surgical architecture for proprioceptive muscle feedback and its potential application to control of advanced limb prostheses," *J Neural Eng,* vol. 14, no. 3, p. 036002, Jun 2017.

[25] T. R. Clites *et al.*, "Proprioception from a neurally controlled lower-extremity prosthesis," *Science Translational Medicine,* vol. 10, no. 443, May 30 2018.

[26] T. R. Clites, H. M. Herr, S. S. Srinivasan, A. N. Zorzos, and M. J. Carty, "The Ewing Amputation: The First Human Implementation of the Agonist-Antagonist Myoneural Interface," *Plastic and Reconstructive Surgery-Global Open,* vol. 6, no. 11, Nov 2018.

[27] D. Burke, K. E. Hagbarth, L. Lofstedt, and B. G. Wallin, "The responses of human muscle spindle endings to vibration of non-contracting muscles," *J Physiol,* vol. 261, no. 3, pp. 673-93, Oct 1976.

[28] O. White and U. Proske, "Illusions of forearm displacement during vibration of elbow muscles in humans," *Exp Brain Res,* vol. 192, no. 1, pp. 113-20, Jan 2009.

[29] P. D. Marasco *et al.*, "Illusory movement perception improves motor control for prosthetic hands," *Sci Transl Med,* vol. 10, no. 432, Mar 14 2018.

[30] K. Horch, S. Meek, T. G. Taylor, and D. T. Hutchinson, "Object Discrimination With an Artificial Hand Using Electrical Stimulation of Peripheral Tactile and Proprioceptive Pathways With Intrafascicular Electrodes," *IEEE Transactions on Neural Systems & Rehabilitation Engineering,* vol. 19, no. 5, pp. 483-489, Oct 2011.

[31] M. Schiefer, D. Tan, S. M. Sidek, and D. J. Tyler, "Sensory feedback by peripheral nerve stimulation improves task performance in individuals with upper limb loss using a myoelectric prosthesis," *Journal of Neural Engineering,* vol. 13, no. 1, Feb 2016.

[32] S. Wendelken *et al.*, "Restoration of motor control and proprioceptive and cutaneous sensation in humans with prior upper-limb amputation via multiple Utah Slanted Electrode Arrays (USEAs) implanted in residual peripheral arm nerves," *Journal of Neuroengineering and Rehabilitation,* vol. 14, Nov 25 2017.

[33] E. D'Anna *et al.*, "A closed-loop hand prosthesis with simultaneous intraneural tactile and position feedback," *Science Robotics,* vol. 4, no. 27, Feb 20 2019.

[34] P. M. Rossini *et al.*, "Double nerve intraneural interface implant on a human amputee for robotic hand control," *Clinical Neurophysiology,* Article vol. 121, no. 5, pp. 777-783, May 2010.

[35] T. S. Davis *et al.*, "Restoring motor control and sensory feedback in people with upper extremity amputations using arrays of 96 microelectrodes implanted in the median and ulnar nerves," *J Neural Eng,* vol. 13, no. 3, p. 036001, Jun 2016.

[36] E. G. Papadopoulos and G. C. Chasparis, "Analysis and model-based control of servomechanism with friction," *in IEEE/RSJ International Conference on Intelligent Robots and Systems, Vols 1-3, Proceedings,* pp. 2109-2114, 2002.

[37] Koukoulas N., Bertos A.G, Mablekos-Alexiou A., and P. E., "A Biomechatronic EPP upper-limb prosthesis teleoperation system implementation using Bluetooth Low Energy," in *40th International IEEE Engineering in Medicine and Biology Conference*, Honolulu, Hawaii, USA, July 17-21, 2018.

[38] P. G. Jung, G. Lim, S. Kim, and K. Kong, "A Wearable Gesture Recognition Device for Detecting Muscular Activities Based on Air-Pressure Sensors," *IEEE Transactions on Industrial Informatics,* vol. 11, no. 2, pp. 485-494, 2015.

[39] D. G. Lloyd and T. F. Besier, "An EMG-driven musculoskeletal model to estimate muscle forces and knee joint moments in vivo," *J Biomech,* vol. 36, no. 6, pp. 765-76, Jun 2003.

[40] D. Meldrum, E. Cahalane, R. Conroy, D. Fitzgerald, and O. Hardiman, "Maximum voluntary isometric contraction: reference values and clinical application," *Amyotroph Lateral Scler,* vol. 8, no. 1, pp. 47-55, Feb 2007.

[41] C. E. Shannon, "A mathematical theory of communication," *The Bell System Technical Journal,* vol. 27, no. 3, pp. 379-423, 1948.

[42] P. M. Fitts, "The information capacity of the human motor system in controlling the amplitude of movement," *Journal of Experimental Psychology,* vol. 47, no. 6, pp. 381-391, 1954.

[43] X. Zhang and I. S. MacKenzie, "Evaluating eye tracking with ISO 9241 - part 9," in *12th Int. Conference on Human-computer Interaction: intelligent multimodal interaction environments,* Beijing, China, 2007.

[44] C. Choi, S. Micera, J. Carpaneto, and J. Kim, "Development and quantitative performance evaluation of a noninvasive EMG computer interface," *IEEE Trans Biomed Eng,* vol. 56, no. 1, pp. 188-91, Jan 2009.

[45] J. Park, W. Bae, H. Kim, and S. Park, "EMG — force correlation considering Fitts’ law," in *2008 IEEE International Conference on Multisensor Fusion and Integration for Intelligent Systems*, 2008, pp. 644-649.

[46] M. R. Williams and R. F. Kirsch, "Evaluation of Head Orientation and Neck Muscle EMG Signals as Command Inputs to a Human–Computer Interface for Individuals With High Tetraplegia," *IEEE Transactions on Neural Systems and Rehabilitation Engineering,* vol. 16, no. 5, pp. 485-496, 2008.

[47] L. H. Smith, T. A. Kuiken, and L. J. Hargrove, "Myoelectric Control System and Task-Specific Characteristics Affect Voluntary Use of Simultaneous Control," *IEEE Trans Neural Syst Rehabil Eng,* vol. 24, no. 1, pp. 109-16, Jan 2016.

[48] E. N. Kamavuako, E. J. Scheme, and K. B. Englehart, "On the usability of intramuscular EMG for prosthetic control: a Fitts' Law approach," *J Electromyogr Kinesiol,* v. 24, n. 5, pp. 770-7, Oct 2014.

[49] I. S. MacKenzie and P. Isokoski, *Fitts' throughput and the speed-accuracy tradeoff*. 2008, pp. 1633-1636.

[50] E. R. F. W. Crossman, "The information-capacity of the human motor-system in pursuit tracking," *The Quarterly Journal of Experimental Psychology,* vol. 12, pp. 1-16, 1960.

[51] A. T. Welford, *Fundamentals of skill* (Fundamentals of skill.). New York, NY, US: Methuen, 1968.

[52] R. William Soukoreff and I. Scott MacKenzie, *Towards a Standard for Pointing Device Evaluation, Perspectives on 27 Years of Fitts' Law Research in HCI*. 2004, pp. 751-789.

[53] A. M. Simon, L. J. Hargrove, B. A. Lock, and T. A. Kuiken, "The Target Achievement Control Test: Evaluating real-time myoelectric pattern recognition control of a multifunctional upper-limb prosthesis," *Journal of rehabilitation research and development,* vol. 48, no. 6, pp. 619-627, 2011.

[54] L. T. Skovgaard, "Applied regression analysis. 3rd edn. N. R. Draper and H. Smith, Wiley, New York, 1998. No. of pages: xvii+706. Price: £45. ISBN 0-471-17082-8," *Statistics in Medicine,* vol. 19, no. 22, pp. 3136-3139, 2000.

[55] E. J. Scheme and K. B. Englehart, "Validation of a Selective Ensemble-Based Classification Scheme for Myoelectric Control Using a Three-Dimensional Fitts' Law Test," *IEEE Transactions on Neural Systems and Rehabilitation Engineering,* vol. 21, no. 4, pp. 616-623, 2013.

[56] E. Moutopoulou, G. A. Bertos, A. Mablekos-Alexiou, and E. G. Papadopoulos, "Feasibility of a biomechatronic EPP Upper Limb Prosthesis Controller," *Conf Proc IEEE Eng Med Biol Soc,* vol. 2015, pp. 2454-7, 2015.

[57] A. B. Ajiboye *et al.*, "Restoration of reaching and grasping movements through brain-controlled muscle stimulation in a person with tetraplegia: a proof-of-concept demonstration," *Lancet,* vol. 389, no. 10081, pp. 1821-1830, May 6 2017.

[58] R. F. Weir, P. R. Troyk, G. A. DeMichele, D. A. Kerns, J. F. Schorsch, and H. Maas, "Implantable myoelectric sensors (IMESs) for intramuscular electromyogram recording," *IEEE Trans Biomed Eng,* vol. 56, no. 1, pp. 159-71, Jan 2009.

[59] P. F. Pasquina *et al.*, "First-in-man demonstration of a fully implanted myoelectric sensors system to control an advanced electromechanical prosthetic hand," *Journal of Neuroscience Methods,* vol. 244, pp. 85-93, Apr 15 2015.

[60] S. Raspopovic *et al.*, "Restoring natural sensory feedback in real-time bidirectional hand prostheses," *Sci Transl Med,* vol. 6, no. 222, p. 222ra19, Feb 5 2014.

[61] M. Ortiz-Catalan, B. Hakansson, and R. Branemark, "An osseointegrated human-machine gateway for long-term sensory feedback and motor control of artificial limbs," *Sci Transl Med,* vol. 6, no. 257, p. 257re6, Oct 8 2014.

[62] T. A. Kuiken, A. K. Barlow, L. J. Hargrove, and G. A. Dumanian, "Targeted Muscle Reinnervation for the Upper and Lower Extremity," *Techniques in Orthopaedics,* vol. 32, no. 2, pp. 109-116, Jun 2017.

[63] C. M. Frost *et al.*, "Regenerative peripheral nerve interfaces for real-time, proportional control of a Neuroprosthetic hand," *J Neuroeng Rehabil,* vol. 15, no. 1, p. 108, Nov 20 2018.

[64] S. Tarantino, F. Clemente, D. Barone, M. Controzzi, and C. Cipriani, "The myokinetic control interface: tracking implanted magnets as a means for prosthetic control," *Sci Rep,* vol. 7, no. 1, p. 17149, December 7, 2017.

[65] A. K. Fontaine, J. L. Segil, J. H. Caldwell, and R. F. F. F. Weir, "Real-Time Prosthetic Digit Actuation by Optical Read-out of Activity-Dependent Calcium Signals in an Ex Vivo Peripheral Nerve," *2019 9th International Ieee/Embs Conference on Neural Engineering (Ner),* pp. 143-146, 2019.